applied total vertical stress, i.e. a value of $\bar{B}$ much in excess of 1.0: indeed, in the Mastemyr foundation the observed values of $\bar{B}$ varied from 1.89 to 2.39. A phenomenon of local failure can also develop in the very last stages of construction of an embankment where type (1) stress paths (Fig. 2) would be followed: if the embankment construction were continued until point F was reached, local failure would develop at this point. In a clay with strain softening characteristics, the development of local failure would produce an effective stress path such as FC and pore pressures would be generated at a rate corresponding to $\bar{B}$ values in excess of 1.0. Such high values of $\bar{B}$ have indeed been observed in the final stages of construction of the failed test sections A in Saint-Alban (La Rochelle *et al.* 1974) and Cubzac-les-Ponts (Vogien 1975); the same phenomenon may also have occurred locally under the Bäckebol test tank (Sällfors 1975) and may be used to explain the high $\bar{B}$ values presented in Table 1.

Heavily Overconsolidated Clays (OCR > 2.5)

As already discussed the low pore pressures generated in the initial phase of construction in heavily overconsolidated clays result in an effective stress path as represented in Fig. 5. The critical vertical effective stress at which the rate of pore pressure generation increases corresponds to point P_1 and is less than the preconsolidation pressure of the clay.

The principles of the limit state theory imply that the effective stresses developed during further loading remain on the limit state surface of the clay, thus following P_1P (unless the shape of this surface is modified when the clay becomes normally consolidated under the P_1 stress condition). In this case the increase in pore pressures should be less than the applied total stress increment so that the vertical effective stress can increase from $\sigma_{1,\text{crit}}'$ to P_c along P_1P. The values of $\bar{B}$ observed for the 8 piezometers located in clays with an OCR in excess of 2.5 tend to confirm this interpretation since they vary between 0.42 and 1.01 around an average of 0.75.

Proposed Method of Predicting Pore Pressures

The analysis of the pore pressures generated during the construction of 30 embankments has confirmed the general validity of the principles resulting from the detailed evaluation of the Saint-Alban case history as presented in Part I of this paper. The addition of data from overconsolidated clays has clearly indicated that the YLIGHT model, developed from the limit state theory by Tavenas and Leroueil (1977), may be used to understand and predict the generation of pore pressures below the center line of embankments built on clay foundations. The observed pore pressure behaviour can be schematized to form the basis for a relatively simple method of pore pressure prediction.

The variation of pore pressure with the applied total vertical stress $\Delta\sigma_1 = I\Delta\gamma H$ during the construction of an embankment is shown in principle on Fig. 6.

For an applied vertical stress $\Delta\sigma_1$ between 0 and the critical value, the pore pressure coefficient $\bar{B}_1$ results from the combined effects of the pore pressure generation in undrained condition and the rapid consolidation associated with the overconsolidated state of the clay foundation. Although clear evidence is difficult to obtain in the field, it is reasonable to evaluate the pore pressure generation in undrained condition from Henkel's equation

$$\Delta u = \beta\Delta\sigma_{\text{oct}} + 3\ \alpha\Delta\tau_{\text{oct}}$$

As for the effect of consolidation during construction, Schiffman's method (1960) may be applied but the correct evaluation of C_v may prove difficult. An indirect evaluation of C_v on the basis of *in situ* permeability tests may yield the best results. In view of uncertainties related to such analysis, an empirical approach based on the data presented herein may be sufficient. At any time the pore pressure in the clay foundation could be computed from

$$\Delta u_1 = \bar{B}_1 I\gamma H_1$$

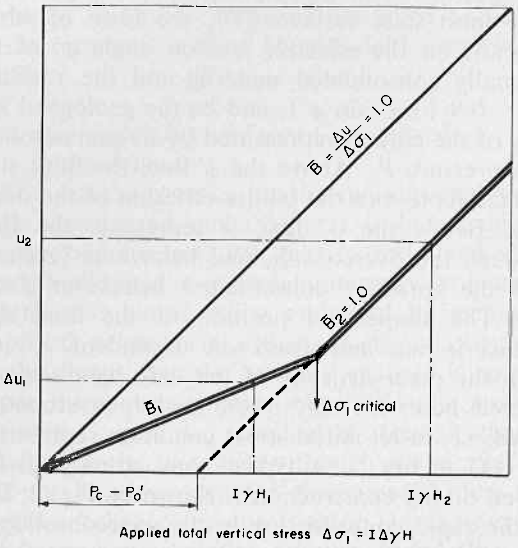

FIG. 6. Schematic variation of the pore pressure with the applied load — principle of the proposed prediction method.